

2014

# Investigating strain transfer in polymer coated structures for the health monitoring of aerospace vehicles using polymer photonic waveguides

Graham Wild  
*RMIT University*

Bronwyn Fox  
*Deakin University*

Kevin Magniez  
*Deakin University*

Steven Hinckley  
*Edith Cowan University, s.hinckley@ecu.edu.au*

Scott Wade  
*Swinburne University of Technology*

*See next page for additional authors*

---

[10.1109/MetroAeroSpace.2014.6865999](https://doi.org/10.1109/MetroAeroSpace.2014.6865999)

This article was originally published as: Wild G., Fox B., Magniez K., Hinckley S., Wade S., & Carman G. (2014). Investigating strain transfer in polymer coated structures for the health monitoring of aerospace vehicles using polymer photonic waveguides. 2014 IEEE International Workshop on Metrology for Aerospace, MetroAeroSpace 2014 - Proceedings. (pp. 622-626). Benevento, Italy. IEEE Computer Society. © 2014 IEEE. Personal use of this material is permitted. Permission from IEEE must be obtained for all other uses, in any current or future media, including reprinting/republishing this material for advertising or promotional purposes, creating new collective works, for resale or redistribution to servers or lists, or reuse of any copyrighted component of this work in other works. Original article available [here](#)

This Conference Proceeding is posted at Research Online.

<http://ro.ecu.edu.au/ecuworkspost2013/45>

---

**Authors**

Graham Wild, Bronwyn Fox, Kevin Magniez, Steven Hinckley, Scott Wade, and G Carman

# Investigating strain transfer in polymer coated structures for the health monitoring of aerospace vehicles using polymer photonic waveguides

Graham Wild

Sir Lawrence Wackett Aerospace Centre  
SAMME, RMIT University  
Melbourne, Australia  
[Graham.Wild@rmit.edu.au](mailto:Graham.Wild@rmit.edu.au)

Steven Hinckley

Centre for Communications Engineering Research  
School of Engineering, Edith Cowan University  
Joondalup, Australia  
[S.Hinckley@ecu.edu.au](mailto:S.Hinckley@ecu.edu.au)

Bronwyn Fox, Kevin Magniez

Institute for Frontier Materials  
Deakin University  
Geelong, Australia  
[bronwyn.fox@deakin.edu.au](mailto:bronwyn.fox@deakin.edu.au),  
[kevin.magniez@deakin.edu.au](mailto:kevin.magniez@deakin.edu.au)

Scott Wade

Centre for Quantum and Optical Science  
Swinburne University of Technology  
Hawthorne, Australia  
[swade@swin.edu.au](mailto:swade@swin.edu.au)

Greg Carman

Department of Mechanical and Aerospace Engineering  
Henry Samueli School of Engineering, UCLA  
Los Angeles, USA  
[carman@seas.ucla.edu](mailto:carman@seas.ucla.edu)

**Abstract**—In this work, we present the concept of planar polymer photonic waveguides for the health monitoring of aerospace structures. Here a polymer layer is deposited onto the material/structure to be monitored. Within the polymer layer, waveguides are created after deposition. These waveguides can then be used as “optical fibres” for optical fibre sensing methodologies. In investigating the use of polymer photonic waveguides the question to be answered is: does the strain in the test material transfer to the polymer layer, such that the value to be measured optically is reliable and indicative of the true strain in the test structure? To answer this question we have conducted a preliminary structural analysis with finite element analysis, utilising ANSYS. A simple aluminium cantilever was used as the test structure, and layers of polyethylene with different thicknesses were added to this. Result show that the thinner the layer of polymer, the more accurate the measured strain will be. For a 100um coating, the difference in strain was observed to be on the order of 3.3%.

**Keywords**—*photonic waveguides; structural health monitoring; strain; stress, finite element analysis; sensing; optical fibre sensing; fibre Bragg grating*

## I. Introduction

The investigation and implementation of Structural Health Monitoring (SHM) systems has been paramount for the monitoring of civil structures such as bridges, buildings and railways [1,2] in practice. SHM involves the monitoring of the mechanical integrity of a structure using a network of sensing elements which can be used to infer the source of damage to the structure and the location of the damage site, in real time, depending on the complexity of the signal processing utilised. The ability to create “smart” structures that alert maintenance engineers to the presence of minor flaws in these materials has the potential to avert disasters and save lives, and significantly reduce operating costs through reduced maintenance and inspection costs. SHM offers a solution to health assessment, safety, maintenance, and management of the structural integrity of aerospace structures.

Despite the success of SHM systems for civil and other mechanical structures, and the potential of the technology to be applied to the monitoring of airframe structures, there has been no penetration of any of the current SHM technologies into the commercial aircraft manufacturing industry. This is despite the fact that these systems have the potential to significantly affect safety and operating costs (through

improvements in maintenance and inspection processes). As such, cost-effective and reliable damage detection in aerospace structures is still difficult to implement and perform. Studies show that 27% of an average aircraft's life cycle cost is spent on inspection and repair [3]. As well as a reduction in maintenance and operating costs of these structures, other benefits include increased lifetime of vehicles and aircraft (contributing to the goal of ageless aerospace vehicles as specified by NASA). The global economic impact in terms of ageing aircraft could be significant. The long term solution for future commercial aviation is an integrated Structural Health Monitoring (SHM) system. The SHM systems proposed are intended to detect and monitor any defects, damage, and faults in-situ during the life cycle of the aerospace structure. Another major goal of these systems is to ensure that structures are safe, and the loss of life associated with infamous aviation incidents [4] does not occur in the future.

Optical fibre sensors are a promising technology, and have been investigated for SHM in aerospace for the past decade [5]. Of particular interest is the optical fibre Bragg grating (FBG) [6]. The FBG offers all of the advantages associated with other optical fibre sensors, whilst being ideally suited to multiplexing (one of the key advantages of the technology) and offering versatility (FBGs can sense almost any measurand with a suitable transducer). FBG have previously been investigated for their use in the SHM of composites [7]. Whilst optical fibres have shown some success in SHM systems for civil structures, and there is intensive research into this technology for aerospace structures, there are still a number of problems associated with this technology. These issues include bonding, embedding, and manufacturing costs. The proposed solution to these issues is the use of planar polymer photonic waveguides in place of traditional optical fibres. This involves the deposition of a polymer layer onto the material to be monitored, with the waveguides created afterwards. The goal of this work is to assess how strain in the test material is transferred to the polymer layer. This will validate if the strain to be measured optically is a true measure of the strain in the test structure.

## II. Theory

To assess the strain transfer from the test material to the polymer layer, a simple static structural analysis of a cantilever beam was used. Using beam theory for a simple cantilever [8], the Von Mises Equivalent Stress ( $\sigma'$ ) can be determined. Assuming plane stress this is given as,

$$\sigma' = \sqrt{(\sigma_x^2 - \sigma_x\sigma_y + \sigma_y^2 + 3\tau_{xy}^2)} \quad (1)$$

Assuming a point load at one end, with the other end fixed, the problem is simplified greatly, given,  $\tau_{xy} = 0$ , and  $\sigma_y = 0$ . That is,

$$\sigma' = \sigma_x \quad (2)$$

The bending stress at the point  $(x, y)$  is then given by,

$$\sigma_x = -\frac{F(L-x)y}{I} \quad (3)$$

where  $F$  is the applied force at the free end of the cantilever (in the  $y$  direction),  $L$  is the length, and

$$I = \frac{bh^3}{12}. \quad (4)$$

Here,  $b$  is the width (perpendicular to the load), and  $h$  is the height (in the direction of the load). The coordinate system is such that  $x$  is zero at the fixed end of the cantilever, and the  $y$  is zero in the middle of the cantilever. The maximum value of  $y$  is then,  $h/2$ . Finally, the strain is then given by,

$$\epsilon_x = \frac{\sigma_x}{E}, \quad (5)$$

where  $E$  is Young's modulus. Substituting (3) and (4) into (5) gives,

$$\epsilon_x = -\frac{12F(L-x)y}{Ebh^3}, \quad (6)$$

From (6) we can determine the strain at any point in the cantilever, as a function of the geometric parameters, the applied load, and Young's modulus. Figure 1 shows the geometry of the cantilever beam, depicting all the parameter, as well as the coordinate system.

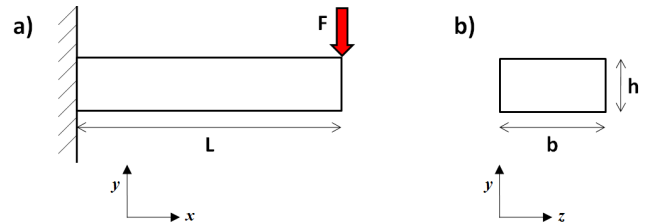


Fig. 1. The geometry of a cantilever beam, along the length (a), and the cross section (b).

## III. Method

A polymer layer was bonded to the upper and lower surface of the cantilever. The system was modelled in ANSYS. The cantilever was made of aluminium, and the polymer was polyethylene. The numerical values of the parameters used in the simulations are shown in Table 1. To assess the effect of the polymer layer, several models were constructed. These had polymer layers up to 0.5mm thick, in 0.1mm increments, from no polymer (giving a total of 6 models). A sample model is illustrated in Figure 2.

TABLE I. PARAMETERS OF THE CANTILEVER BEAM

Property	symbol	Value	Units
Load	$P$	10	N
Length	$L$	25	mm
Width	$b$	20	mm
Height	$h$	5	mm
Young's modulus	$E$	$71 \times 10^9$	Pa

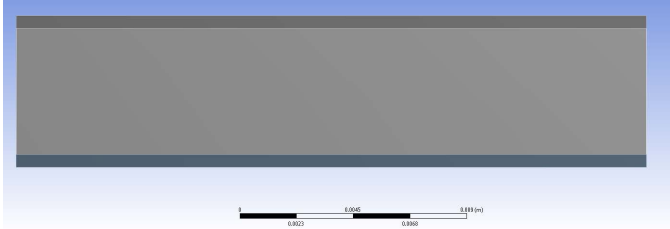


Fig. 2. The cross section of the cantilever, with a 0.5mm thick layer of polyethylene above and below the 5mm thick aluminium

The stress along the cantilever was investigated first, to compare the beam theory to the simulation results, specifically to determine where along the length the strain should be investigated. Next the stress through beam was measured to validate the beam theory. Following this, the strain was then measured at the ideal location, on the surface of the aluminium, and the inner and outer surface of the polyethylene, giving three strain values for each model. Finally, the applied load was varied to assess the effect this had on the strain in the polymer layer. This was performed using the model with the 0.5mm thick polyethylene.

#### iv. Results

The output of the static structural analysis is show in Figure 3. This is at the mid-plane of the width of the cantilever, that is,  $b/2$ . The stress along the surface (upper or lower) of the cantilever is shown in Figure 4. This data was sampled at 32 points along the 25mm length of the cantilever, at the midpoint of the  $y$  axis, corresponding to nodes of the mesh. Along with this data, the result of (3) is also plotted, as the theoretical line.

Next, the stress through the cantilever was measured. Again, the nodes of the mesh along the middle of the cantilever were used as reference points. As such, 8 data points for the internal stress are shown in Figure 5. The theoretical values from (6) are also plotted for comparison.

Once the appropriate location was selected, the strain was determined. For the aluminium cantilever, the strain at the (17.75, 2.5) mm coordinate was  $12.276 \mu\epsilon$ , while the theoretical value from (3) was  $12.267 \mu\epsilon$ . Following this, the polyethylene layers were added, in 0.1mm increments. A sample strain distribution from the FEA is shown in Figure 6. The results for the measured strain from the surface of the aluminium, the inside of the polyethylene layer, and the outside of the polyethylene layer, are shown in Figure 7.

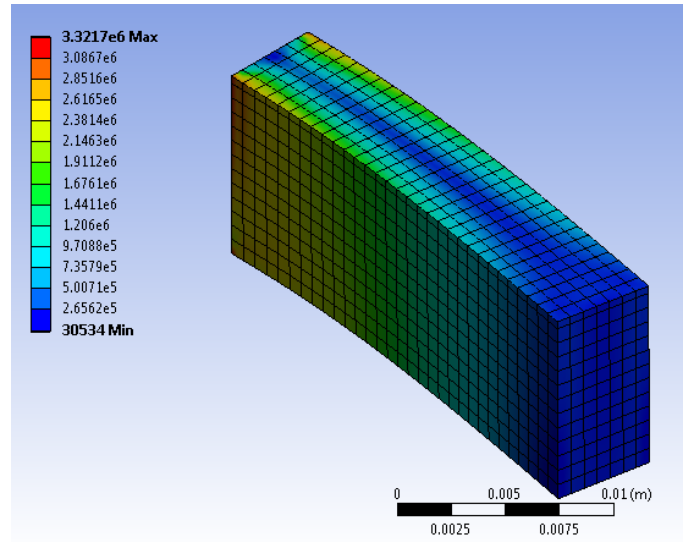


Fig. 3. Static structural analysis result, showing the Von Mises equivalent stress along the cantilever, in the midplane ( $z = b/2$ ).

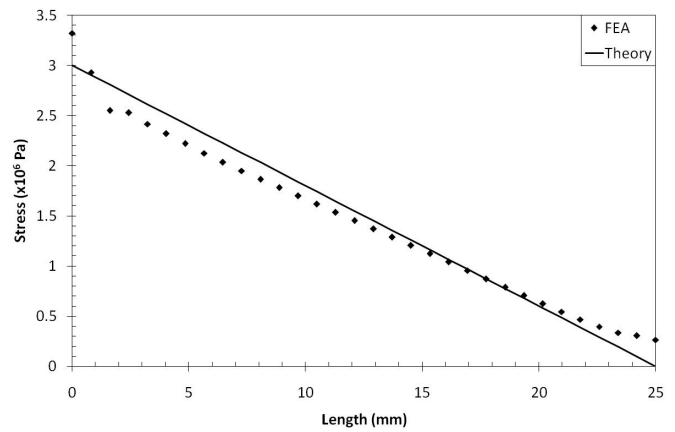


Fig. 4. Von Mises equivalent stress at the surface ( $y = h/2$ ), at the midplane ( $z = b/2$ ), along along the length of the cantilever, from the FEA, and the theoretical value.

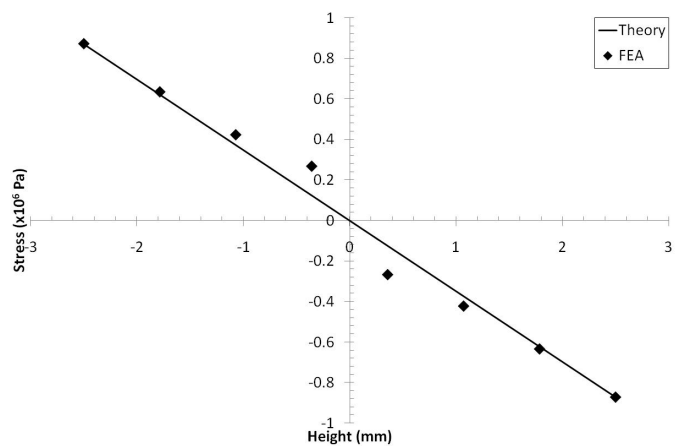


Fig. 5. Stress through the height of the cantilever at the midplane in the  $z$  direction, and with  $x = 17.75$ mm.

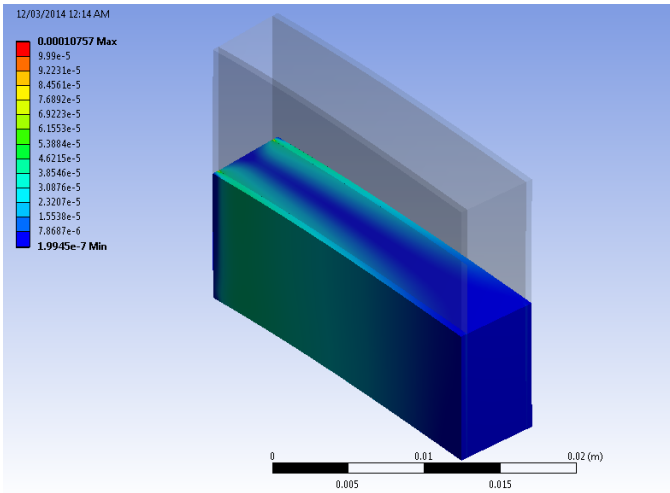


Fig. 6. The strain distribution in the midplane of the 0.5mm polyethylene clad aluminium cantilever.

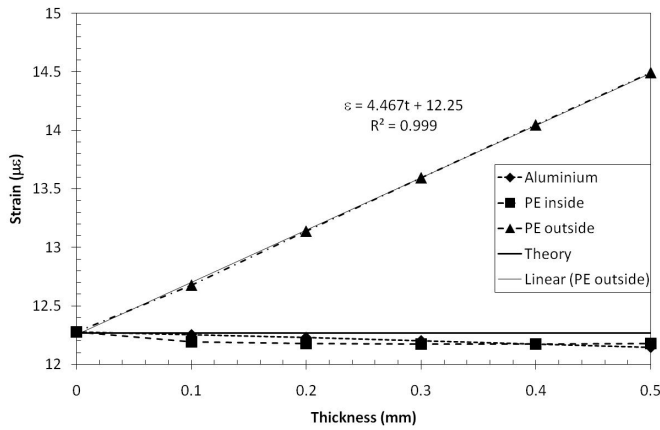


Fig. 7. The strain as a function of the polyethylene layer thickness.

Figure 8 shows strain as a function of the applied load. Again the coordinate used was (17.75, 2.5) mm. The strain was measured at the surface of the aluminium and at the outer layer of the polyethylene. The theoretical values as predicted by (6) were also plotted. Combining the results from Figure 7 and Figure 8 we can show how the applied load and thickness combine to give the strain. The results of this are shown in Figure 9.

## v. Discussion

Figure 4 shows that the FEA model agrees with the theoretical value at an  $x$  coordinate of approximately 17.75mm. The reason that the theoretical line does not agree with all of the FEA values is likely due to the dimensions of the cantilever. That is, the cantilever modelled does not have the aspect ratio of a typical bending system, and the assumptions used to derive the simple theory are not

completely accurate. In this case, the FEA model results are more accurate. The dimensions were chosen based on the fact that a suitable mesh with a reasonable number of elements was required, and there is a limit in the aspect ratio of the individual elements themselves. That is, a 5:1 aspect ratio should not be exceeded for elements in the mesh. As such, the 0.1mm thickness of the polyethylene layer then places limits on the overall dimensions of the structure. With a suitable computer a larger structure could be modelled; however, the findings will not change, just the agreement with the idealised theory.

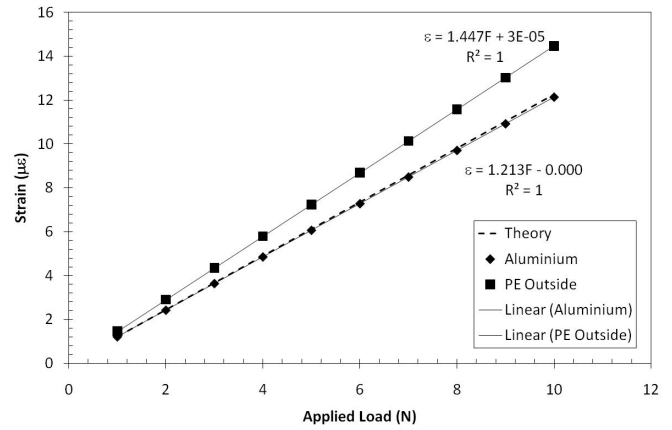


Fig. 8. The strain as a function of the applied load.

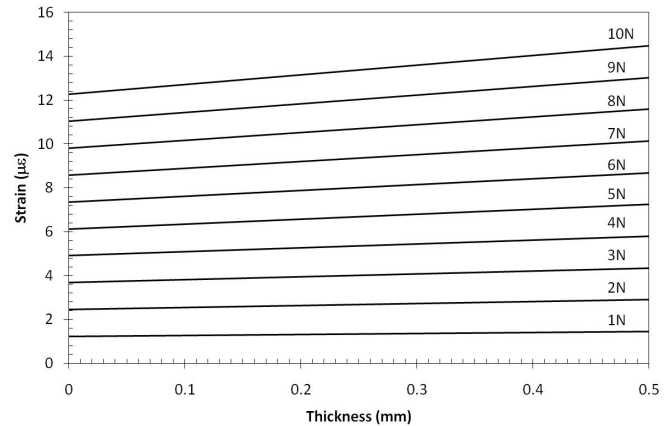


Fig. 9. The strain as a function of polyethylene layer thickness and applied load.

From Figure 5, the results show that the measured values from the simulation agree with those of the simple beam bending theory. As such, the coordinate (17.75, 2.5) selected was an ideal reference point to utilise on the surface of the aluminium cantilever for the strain measurements.

The results in Figure 7 show that the strain at the surface of the aluminium is almost equivalent to the strain on the inner surface of the polyethylene. This result suggests that ignoring bonding issues between the aluminium and polyethylene, the strain stain transfer is idea for the purpose of utilising the polyethylene layer to measure the strain in the test structure. Figure 7 also shows that the thicker the polymer layer, the greater the strain at the outer surface. Specifically, there is a linear relationship between the thickness and the strain, such that a 1 millimetre thick layer of polyethylene would have  $4.467\mu\epsilon$  more strain on the outer surface relative to the inner surface. From this, we can determine a condition to limit the systematic error in any strain measurement.

The final step was to assess the effect of increasing the loading force, to determine if this affected the sensitivity of the strain increase through the polymer layer. From Figure 9 we can see that the sensitivity of the sensing layer as a function of thickness, increases with the applied load (show as the increase in the slot from the 1N at the bottom to the 10N at the top). The important aspect of this feature is that the thickness of the waveguide sensing region needs to be controlled precisely to minimise errors associated with the variation in sensitivity relative to the thickness.

## VI. Future Work

Following this stage in the research project (the modelling phase) experimental verifications will take place. This will involve measuring strain using traditional methodologies at the surface of a test structure, and then on top of an added polymer layer. This will allow for the effect of bonding between the test structure and the polymer layer to be investigated. As polyethylene will probably not adhere to the aluminium substrate very well, an epoxy resin will be used. To facilitate comparison, simulations will be repeated using the appropriate polymer materials. For example, epoxy Novolak resin polymer has been investigated for use as polymer waveguides [9], this should bond well to the aluminium. Other materials will be investigated, looking specifically at the bonding.

In general, this work represents the first stage in a much larger research project. The goal of the project is the development and testing of polymer optical waveguides for use in the SHM of aerospace vehicles. This represents a paradigm shift in the optical metrology utilised in proposed SHM technologies. The fundamental limitation of utilising optical fibres in commercial aerospace vehicles for SHM is in the incorporation of the technology into manufacturing process. That is, in experimental test beds, one off structures, the manual addition of optical fibres to an aerospace structure is common in research. In terms of real application, when we look at the Nishant UAV [10], which uses arrays of optical fibre Bragg gratings for SHM purposes, this is a very low

scale production, with highly labour intensive processes to incorporate the SHM fibres into the aerospace structure. Full scale production of large transport category aircraft will require a technology that can be easily incorporated into the fabrication process of the aerospace vehicle. The prospect to then add an additional polymer layer, and inscribe waveguides into this, is far more viable than manually laying up glass optical fibres. This research project will test this hypothesis, to determine if polymer optical waveguides represents a more viable technological solution to conventional optical fibre based SHM.

## VII. Conclusion

In conclusion, we have demonstrated that the strain in a mechanical structure is efficiently transferred into a coupled polymer layer. The thinner the layer, the more closely the strain through its cross section is equal to that at the surface of the mechanical structure. That is, the thicker the polymer layer, the greater the variation in the strain to the outer surface relative to the inner surface. This result means that the coupled polymer layer can be used to measure the strain in the mechanical structure. As such, the proposed polymer photonic waveguides will facilitate the integration of structural health monitoring technologies into large scale airframe manufacturing, to increase the service life of future aerospace vehicles.

## References

- [1] Chang, PC, Faltau, A, & Liu, SC. "Review Paper: Health Monitoring of Civil Infrastructure." *Structural Health Monitoring*, 2(3), 257-267 (2003).
- [2] Farrar, CR & Worden, K. "An introduction to structural health monitoring." *Phil. Trans. R. Soc. A*, 365(1851) 303-315 (2007).
- [3] Hall, SR & Conquest, TJ. "The total data integrity initiative- structural health monitoring, the next generation." *Proceedings of the USAF ASIP Conference*, 1999. 2nd ed.
- [4] Note: See for example, Aloha Airlines Flight 243.
- [5] Staszewski, WJ, Boller, C, & Tomlinson GJ. *Health Monitoring of Aerospace Structures: Smart Sensor Technologies and Signal Processing*, John Wiley & Sons (2004)
- [6] Rao, YJ. "Recent progress in applications of in-fibre Bragg grating sensors." *Opt. Laser. Eng.*, 31(4) 297-324 (1999)
- [7] Emmons, MC, Karnani, S, Trono, S, Mohanchandra, KP, Richards, L, & Carman, GP. "Strain measurement validation of embedded fiber Bragg gratings." *Int. J. of Optomechatronics*, 4(1) 22-33 (2010).
- [8] Hibbeler, RC. *Engineering Mechanics: Statics*, 12th eds, Prentice Hall (2010)..
- [9] Wong, WH, Zhou, J, & Pun, EYB. "Low-loss polymeric optical waveguides using electron-beam direct writing." *Appl. Phys. Lett.* 78(15), 2110 (2001)
- [10] Smart Fibres Ltd "Nishant UAV SHM: In-flight monitoring of strain in the structure of Nishant UAV". Smart Fibres Project Reference Paper (No Date)